Nanocapsules Hot Paper

International Edition: DOI: 10.1002/anie.201602745
German Edition: DOI: 10.1002/ange.201602745

Hollow Carbon Nanobubbles: Synthesis, Chemical Functionalization, and Container-Type Behavior in Water

*Corinne J. Hofer, Robert N. Grass, Martin Zeltner, Carlos A. Mora, Frank Krumeich, and Wendelin J. Stark**

Abstract: *Thin-walled, hollow carbon nanospheres with a hydrophobic interior and good water dispersability can be synthesized in two steps: First, metal nanoparticles, coated with a few layers of graphene-like carbon, are selectively modified on the outside with a covalently attached hydrophilic polymer. Second, the metal core is removed at elevated temperature treatment with acid, leaving a well-defined carbon-based hydrophobic cavity. Loading experiments with the dye rhodamine B and doxorubicin confirmed the filling and release of a cargo and adjustment of a dynamic equilibrium (cargo-loaded versus release). Rhodamine B preferably accumulates in the interior of the bubbles. Filled nanobubbles allowed constant dye release into pure water. Studies of the concentration-dependent loading and release show an unusual hysteresis.*

Capsule systems have attracted tremendous attention in the areas of catalysis and biomaterials, as electrode materials,[1] and for the encapsulation of sensitive materials (therapeutics,[2] fluorescent markers,[3] and others[4]). Inorganic hollow spheres have been prepared from metals, alloys, and oxides (Table S1, entries 1–14, in the Supporting Information).[1b,5] Polymer capsules can be synthesized by layer-by-layer (LbL) adsorption,[1a,6] self-assembly of amphiphilic molecules,[1c,7] from double emulsions,[8] or by polymerization,[9] such as surface-initiated polymerization and crosslinking[10] with subsequent removal of the templating core (Table S1, entries 15–22).

Undoubtedly the most prominent example of a carbon capsule is fullerene, in particular buckminsterfullerene (C_{60})[11] whose basic structural element is related to graphene.[12] The C_{60} central cavity (0.71 nm in diameter) has been used to enclose lanthanum,[13] noble gases,[14] nitrogen,[15] phosphorus,[16] hydrogen,[17] and water[18] by ion implantation or by chemical opening and closing (endohedral fullerenes). The limited space (few atoms per C_{60}) and the difficult fill/release processes, however, do not permit a real container/cargo function. The interior of bigger, fullerene-like graphitic capsules (3–10 nm), consisting of few onion-like oriented graphene layers, is inaccessible for organic molecule cargos (Table S1, entries 23–25).[19]

Carbon capsules can be produced by carbonization of polymer shells at high temperatures,[20] by hydrothermal[21] or solvothermal methods[22] and by "confined nanospace pyrolysis".[2c,23] They often have a low degree of graphitization and consist mainly of amorphous carbon (Table S1, entries 27–42). Carbon capsules having a higher graphitization degree are often made from either radially oriented graphitic sheets or spherically arranged graphitic sheets. The latter contain numerous openings and therefore are rather loosely associated flakes than closed shells.[24] During the carbonization process the well-defined chemical structure of the carbon precursor is lost. Therefore, carbon shells often have the same hydrophobic surface inside as well as outside.[24] For most applications as a container, however, a hollow nanosphere should carry a hydrophobic cargo through an aqueous environment, that is, the nanocapsule has chemically different inner and outer surfaces.

We therefore developed a water-dispersible, covalently functionalized, highly graphitic carbon nanocapsule with a hydrophobic interior as outlined in Figure 1. In contrast to other carbon capsules the hollow carbon nanobubbles presented here consist of a closed shell of three to four layers of sp^2-hybridized carbon and thus are highly graphitic.[25] With this synthesis method, it is furthermore possible to obtain hollow spheres with chemically well-defined different inner and outer surfaces. The synthesis starts from carbon-coated cobalt metal nanoparticles (C/Co)[26] about 31 ± 20 nm in diameter[27] in which the shell consists of the three to four layers of sp^2-hybridized carbon. A negatively charged polymer was grown directly from the particles by surface-initiated

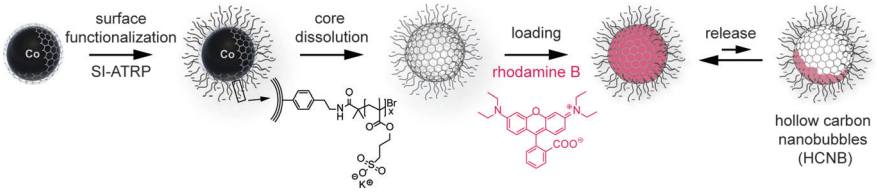

Figure 1. Synthesis, loading, and release of hollow carbon nanobubbles. They are synthesized by surface functionalization of carbon-coated cobalt nanoparticles to achieve favorable surface properties and subsequentcore removal. The nanobubbles can be loaded with substrates which afterwards can be steadily released.

[*] M. Sc. C. J. Hofer, Dr. R. N. Grass, Dr. M. Zeltner, M. Sc. C. A. Mora, Dr. F. Krumeich, Prof. Dr. W. J. Stark
Institute for Chemical and Bioengineering, ETH Zurich
Vladimir-Prelog-Weg 1, 8093 Zurich (Switzerland)
E-mail: wendelin.stark@chem.ethz.ch

Supporting information for this article can be found under: http://dx.doi.org/10.1002/anie.201602745.

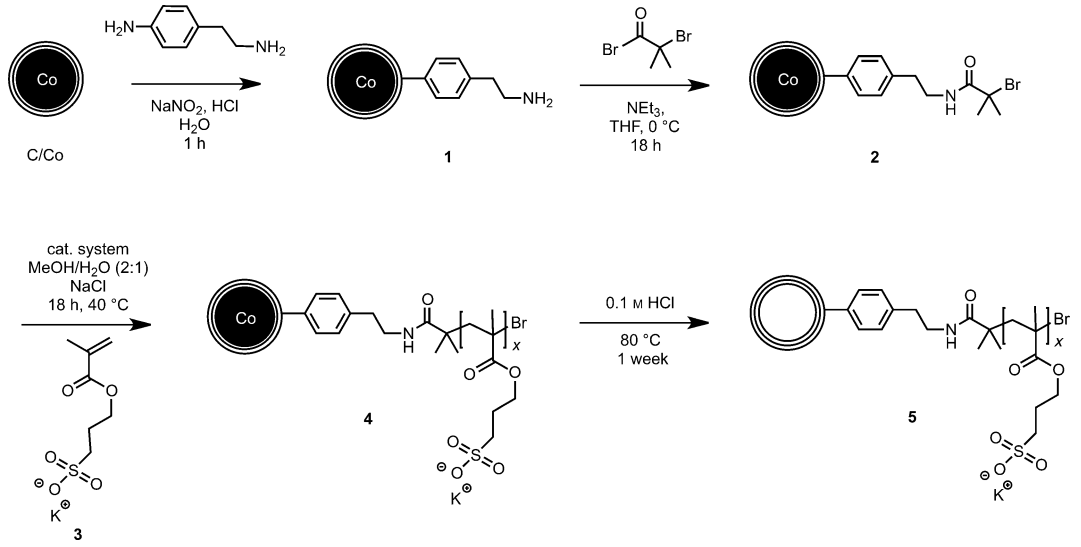

Scheme 1. Covalent surface functionalization of carbon-coated cobalt nanoparticles (C/Co) and subsequent formation of hollow carbon nanobubbles (HCNB, **5**). Diazonium chemistry (**1**) and amidation were used to generate an initiator (**2**) for SI-ATRP of 3-sulfopropyl methacrylate potassium salt (SPM, **3**) to yield **4**. Subsequent dissolution of the templating cobalt core under acidic conditions and elevated temperature yields hollow carbon nanobubbles (HCNB, **5**). Cat. system: copper(II) bromide ($CuBr_2$), 2,2′-bipyridine, L-ascorbic acid.

atom transfer radical polymerization (SI-ATRP) to introduce steric and electrostatic repulsion (Scheme 1 and the Supporting Information).[27] The metal core enables the selective surface functionalization of the outer capsule wall and furthermore simplifies both surface functionalization and sample purification since it is magnetic.[28] The templating metal core was then selectively removed by acidic dissolution at elevated temperature. This is possible because of physical defects in the graphene shells.[29] The procedure presented here allows the formation of highly graphitic carbon shells without loss of the chemically well-defined outer surface structure. Under the conditions used (0.1M HCl, 80°C, 1 week) about 77% of the particles could be emptied (Tables S2 and S3). After workup pure nanobubbles in yields ranging from 2% to 49% were obtained (Figures S1 and S2 and Table S3).

Electron microscopy images confirmed the successful dissolution of the cobalt metal core and preparation of the nanobubbles (Figure 2 and Figures S3 and S4). The hollow carbon shells, which are 33 ± 16 nm in diameter (Figure S5) and consist of carbon layers and the surrounding polymer layer, are visualized in Figure 2e and Figure S4. The presence of sulfur in the shell wall (sulfonate groups) was detected by energy-dispersive X-ray spectroscopy (EDX), elemental microanalysis, and infrared spectroscopy and further confirms that the polymer did not degrade during the core dissolution process (Figures S7 and S8 and Table S4). The hollow carbon nanobubbles have a zeta potential of −40.5 mV in water. This is again in line with the sulfonate-containing polymer and the nanobubbles' good dispersability in water. The successful core dissolution was additionally proven by X-ray diffraction spectroscopy (reduction of cobalt metal content in the samples), elemental microanalysis (relative increase in carbon content), and thermogravimetric analysis (altered oxidation profile and ash content, see Figure S9, Table S5, and Figure S10).

To investigate the accessibility of the bubble interior, the nanobubbles were loaded with rhodamine B using an aqueous dye solution (detailed procedure in the Supporting Information). UV/Vis spectra of solutions containing i) nanobubbles loaded with rhodamine B and ii) the same amount of rhodamine B in free solution showed that the absorption signal is

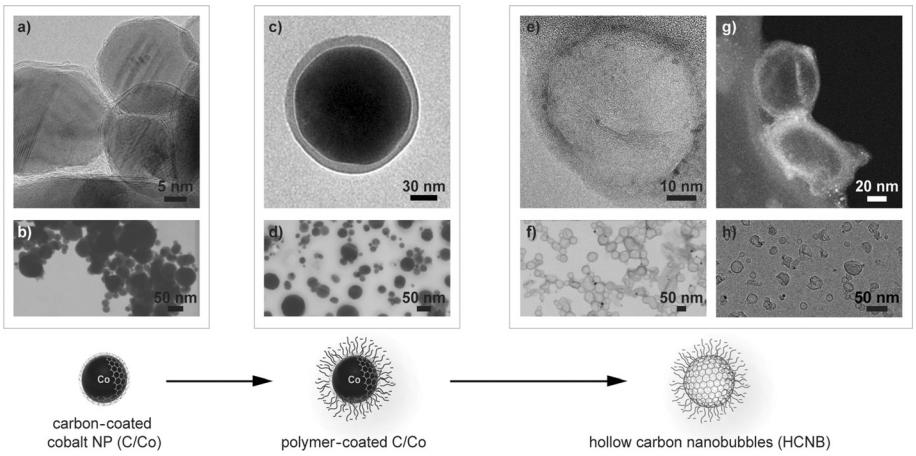

Figure 2. Transmission (TEM) and scanning transmission electron micrographs (STEM) of unfunctionalized carbon-coated cobalt nanoparticles (C/Co, a and b), surface-functionalized carbon-coated cobalt nanoparticles (**4**, c and d) and hollow carbon nanobubbles (**5**, e and f) as well as HAADF-STEM (g) and cryo-TEM (h) of nanobubbles (**5**).

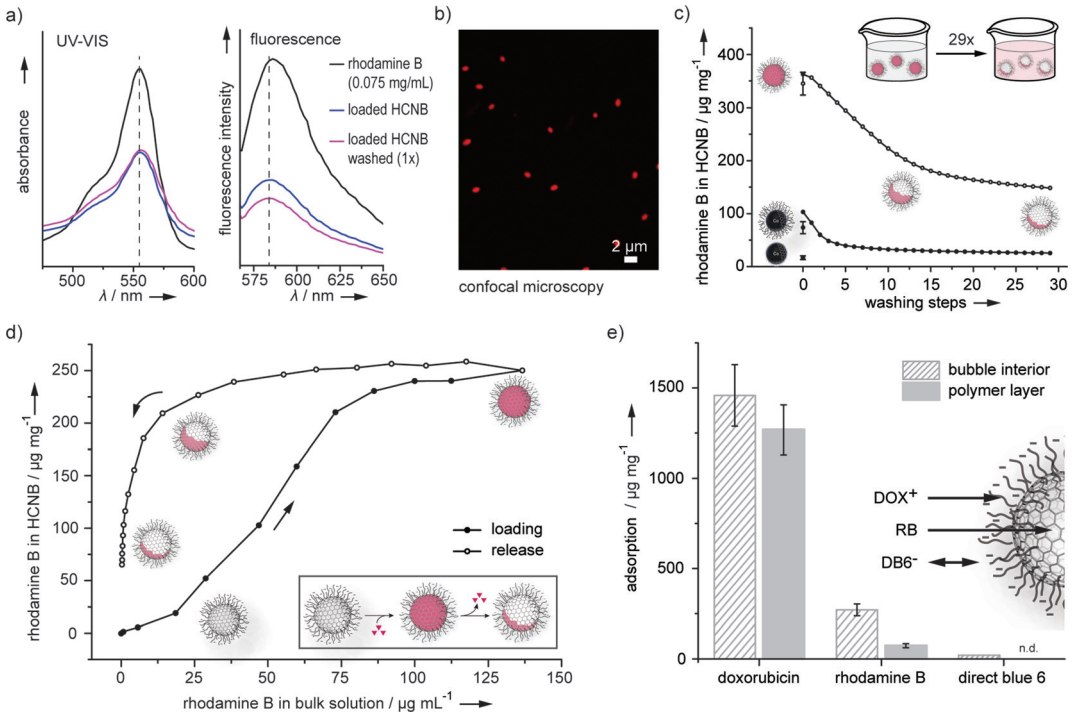

Figure 3. Loading and release of different cargos in hollow carbon nanobubbles (HCNB). a) UV/Vis and fluorescence emission spectra (excitation wavelength: 540 nm) of free rhodamine B (concentration: 0.075 mg mL^{-1}), nanobubbles with encapsulated rhodamine B (measured concentration: 0.076 mg mL^{-1}), and the same nanobubbles after washing (measured concentration: 0.074 mg mL^{-1}). b) Confocal fluorescence microscopy of hollow carbon nanobubbles filled with rhodamine B. c) Rhodamine B release by stepwise removal of released rhodamine B in the bulk solution. d) Loading and release behavior of rhodamine B in hollow carbon nanobubbles by variation of the rhodamine B concentration in the bulk solution. e) Loading of doxorubicin (DOX^+), rhodamine B (RhB), and direct blue 6 ($DB6^-$) into hollow carbon nanobubbles; n.d.: not detectable.

lower for encapsulated rhodamine B (Figure 3a). To confirm that the rhodamine B is located inside the nanobubbles, the capsules were washed by adding water, shaking, and subsequently collecting by filtration. No significant decrease of the UV/Vis signal of the washed nanobubbles is observed which means that only minor amounts of rhodamine B were lost. Fluorescence spectroscopy revealed signal quenching for encapsulated rhodamine B and a slight peak shift (Figure 3a).[30] The presence of rhodamine B in the nanobubbles is further in line with confocal fluorescence microscopy images (Figure 3b and Figure S13). From UV/Vis measurement of the supernatant after filtration of the freshly loaded nanobubbles, an average amount of 345 ± 21 µg of rhodamine B per mg of nanobubbles was calculated (Figure 3c). This was shown to correspond to the saturation adsorption amount (see Figure S14). As an independent proof that rhodamine B is really located inside the nanobubbles and not simply adsorbed on the polymer layer, nanobubbles filled with metal (**4**, that is, the same material but without the hollow interior, since the metal occupies the interior) were used as a control. For this, samples of equivalent surface area were compared, meaning that in the experiment five times more C/Co than nanobubbles (based on the weight) had to be used in order to achieve roughly the same number of spheres in all samples (unfunctionalized C/Co, functionalized C/Co and nanobubbles). Some rhodamine B is indeed adsorbed on the outside of the capsules (see Figure 3c); however this amount is small. The ratio of mass per volume inside the nanobubbles is 0.78 g rhodamine B per mL, which is formally equivalent to a concentration (see the Supporting Information for calculations). The inside concentration is about 10000 times higher than that in the bulk aqueous phase surrounding the nanobubbles. To achieve such a high local rhodamine B concentration it has to move from a low- to a high-concentration region. A similar self-accumulating effect of rhodamine B has already been observed in a study on aged polyelectrolyte microcapsules, where electrostatic interactions were the driving force.[31] In the present work, a possible driving force may be related to the hydrophobicity of the graphene-like inside wall of the nanobubbles. Indeed, rhodamine B is poorly soluble in water (15 g L^{-1} at 20 °C) and it is hydrophobic as indicated by the octanol/water (OW) partition coefficient ($K_{ow} = 190$[32]). This may explain why it accumulates in the hydrophobic environment of the sphere's interior. In analogy to the octanol/water two-phase system, rhodamine B accumulates in the hydrophobic phase. Obviously, there is no real two-phase system but rather a mixture of nanosized hydrophobic cavities in water. Comparison of the specific surface-area-related adsorption capacity of rhodamine B on various carbon-based adsorbents reveals that the adsorption capacity of these hollow carbon nanobubbles is high. This further indicates that rhodamine B is not just adsorbed on the surface but accumulates in the hydrophobic interior of the bubbles (Table S7).

The release behavior was investigated by repeated washing of the nanobubbles with pure water (Figure 3c, detailed

description in the Supporting Information). It was observed that for each of the first 10 washing steps, approximately the same amount of rhodamine B was released (3.3 $\mu g\,mL^{-1}$, see Figure S15). This is in line with the presence of a dynamic equilibrium between the bubble's interior and the bulk, resulting in a concentration-controlled release of rhodamine B (see Figure S16). In other words, the substance is only released from the nanobubbles when it is removed or consumed; this property may be used for drug-delivery applications to achieve constant drug concentration over prolonged periods of time.

To obtain better insight, concentration-dependent loading and release experiments were performed. Nanobubbles were subsequently exposed to aqueous solutions with increasing and then decreasing concentrations of rhodamine B in water (Figure 3d). Astonishingly, the results show a hysteresis in loading and release, confirming that the system not only depends on the input parameter but also on its history. This behavior is known from physical adsorption isotherms of Type IV (IUPAC classification) which occurs for strong fluid–wall forces when the material is mesoporous and capillary condensation occurs.[33] Another effect causing such similar sorption hysteresis is known from mercury porosimetry, where pore size is determined by mercury adsorption. During the extrusion process, new mercury interfaces have to be created, which requires additional energy. If this energy is overcome a sudden retreat of the mercury from a specific pore is observed; this is known as the "snap-off" effect.[34] For the system here the observed hysteresis in loading and release might arise from the hydrophobicity in the bubble interior. Rhodamine B accumulates in the bubbles and forms a droplet, somehow corresponding to that in an O/W emulsion. In this droplet rhodamine B is in a rather stable state and a low bulk concentration is needed to start the release. Once the release started, a "snap-off" effect can be observed (see Figure S18).

Besides rhodamine B, doxorubicin, one of the most widely used commercial drugs for the treatment of breast cancer, can be loaded into the hollow carbon nanobubbles ($2727 \pm 37\,\mu g\,mg^{-1}$, see the Supporting Information for a detailed description). Because of its high toxicity, several works investigated suitable methods for the delivery of doxorubicin.[2c,35] The amount loaded in the bubble interior is $1459 \pm 170\,\mu g\,mg^{-1}$ (Figure 3e). For doxorubicin, the adsorption capacity per specific surface area of the nanobubbles is high when compared to that of other carbon-based adsorbents (see Table S8). It should be noted that in our case almost half of the adsorbed doxorubicin is adsorbed in the polymer shell. This is not surprising when one considers that the cargo molecule has to first diffuse through the polymer shell before it can enter the carbon shell through one of its defects (see Figure S19). In contrast to rhodamine B, which is a zwitterion under the conditions used and therefor overall neutral in charge, positively charged doxorubicin can interact electrostatically with the negatively charged polymer shell. Direct blue 6, which is negatively charged, cannot be loaded to the bubbles' interior and is also not adsorbed in the polymer shell. This is in accordance with the previously mentioned interaction between the polymer shell and the cargo molecule, which in this case is repulsive due to the cargo's negative charge; this makes the loading of direct blue 6 into the bubbles impossible (Figure 3e).

In summary, we have shown how the metal core of carbon-coated nanoparticles can be selectively removed to prepare carbon nanobubbles with defined loading and release properties. Selective covalent chemical derivatization of the carbon shells' exterior permits highly stable dispersion in water while the hydrophobicity of the interior makes it possible to accommodate cargo. The loading of differently charged cargos into the bubbles permitted a general insight on the dependence of the loading on the cargo molecule's charge. The procedure therefore extends the encapsulation of single atoms or molecules in fullerenes to a larger cavity. Owing to the well-defined chemical integrity of the bubbles, their fascinating properties as refillable nanocarriers (e.g. liposomes) can be transferred to chemically demanding environments. Conceptually, a carbon-based nanobubble having a hydrophilic exterior and a hydrophobic structurally coherent interior can be considered to be a micelle (Figure 1 right). The mechanical stability allows the formation of stable emulsions with unlimited lifetimes.

Acknowledgements

Financial support was provided by ETH Zurich, Switzerland. We acknowledge support from the Scientific Center for Optical and Electron Microscopy (ScopeM) of the Swiss Federal Institute of Technology (ETHZ) for confocal microscopy and cryo-TEM and Simon Andrea Nüssli for experimental support.

Keywords: capsules · graphene · hydrophobic interactions · hysteresis · nanostructures

How to cite: *Angew. Chem. Int. Ed.* **2016**, *55*, 8761–8765
Angew. Chem. **2016**, *128*, 8905–8909

[1] a) F. Caruso, *Chem. Eur. J.* **2000**, *6*, 413; b) X. W. Lou, L. A. Archer, Z. C. Yang, *Adv. Mater.* **2008**, *20*, 3987; c) C. S. Peyratout, L. Dähne, *Angew. Chem. Int. Ed.* **2004**, *43*, 3762; *Angew. Chem.* **2004**, *116*, 3850; d) P. F. Zhang, Z. A. Qiao, S. Dai, *Chem. Commun.* **2015**, *51*, 9246; e) A. H. Lu, W. C. Li, G. P. Hao, B. Spliethoff, H. J. Bongard, B. B. Schaack, F. Schüth, *Angew. Chem. Int. Ed.* **2010**, *49*, 1615; *Angew. Chem.* **2010**, *122*, 1659.

[2] a) Y. Ping, J. L. Guo, H. Ejima, X. Chen, J. J. Richardson, H. L. Sun, F. Caruso, *Small* **2015**, *11*, 2032; b) V. Sokolova, M. Epple, *Angew. Chem. Int. Ed.* **2008**, *47*, 1382; *Angew. Chem.* **2008**, *120*, 1402; c) L. M. Wang, Q. Sun, X. Wang, T. Wen, J. J. Yin, P. Y. Wang, R. Bai, X. Q. Zhang, L. H. Zhang, A. H. Lu, C. Y. Chen, *J. Am. Chem. Soc.* **2015**, *137*, 1947; d) Y. F. Zhu, J. L. Shi, W. H. Shen, X. P. Dong, J. W. Feng, M. L. Ruan, Y. S. Li, *Angew. Chem. Int. Ed.* **2005**, *44*, 5083; *Angew. Chem.* **2005**, *117*, 5213.

[3] a) G. Sukhorukov, L. Dähne, J. Hartmann, E. Donath, H. Mohwald, *Adv. Mater.* **2000**, *12*, 112; b) D. H. M. Buchold, C. Feldmann, *Nano Lett.* **2007**, *7*, 3489.

[4] a) D. G. Shchukin, G. B. Sukhorukov, H. Möhwald, *Angew. Chem. Int. Ed.* **2003**, *42*, 4472; *Angew. Chem.* **2003**, *115*, 4610; b) Y. J. Wang, F. Caruso, *Chem. Mater.* **2005**, *17*, 953.

[5] H. Gröger, C. Kind, P. Leidinger, M. Roming, C. Feldmann, *Materials* **2010**, *3*, 4355.

[6] F. Caruso, R. A. Caruso, H. Möhwald, *Science* **1998**, *282*, 1111.

[7] J. Z. Du, R. K. O'Reilly, *Soft Matter* **2009**, *5*, 3544.
[8] S. Cohen, T. Yoshioka, M. Lucarelli, L. Hwang, R. Langer, *Pharm. Res.* **1991**, *8*, 713.
[9] a) B. Y. Li, X. J. Yang, L. L. Xia, M. I. Majeed, B. Tan, *Sci. Rep.* **2013**, *3*, 6; b) G. D. Fu, G. L. Li, K. G. Neoh, E. T. Kang, *Prog. Polym. Sci.* **2011**, *36*, 127.
[10] a) G. D. Fu, Z. H. Shang, L. Hong, E. T. Kang, K. G. Neoh, *Adv. Mater.* **2005**, *17*, 2622; b) G. J. Guan, Z. P. Zhang, Z. Y. Wang, B. H. Liu, D. M. Gao, C. G. Xie, *Adv. Mater.* **2007**, *19*, 2370; c) X. L. Xu, S. A. Asher, *J. Am. Chem. Soc.* **2004**, *126*, 7940.
[11] H. W. Kroto, J. R. Heath, S. C. O'Brien, R. F. Curl, R. E. Smalley, *Nature* **1985**, *318*, 162.
[12] A. K. Geim, K. S. Novoselov, *Nat. Mater.* **2007**, *6*, 183.
[13] J. R. Heath, S. C. O'Brien, Q. Zhang, Y. Liu, R. F. Curl, H. W. Kroto, F. K. Tittel, R. E. Smalley, *J. Am. Chem. Soc.* **1985**, *107*, 7779.
[14] M. Saunders, H. A. Jimenezvazquez, R. J. Cross, R. J. Poreda, *Science* **1993**, *259*, 1428.
[15] T. A. Murphy, T. Pawlik, A. Weidinger, M. Höhne, R. Alcala, J. M. Spaeth, *Phys. Rev. Lett.* **1996**, *77*, 1075.
[16] A. Weidinger, B. Pietzak, M. Waiblinger, K. Lips, B. Nuber, A. Hirsch in *Electronic Properties of Novel Materials—Progress in Molecular Nanostructures: Xii International Winterschool, Vol. 442* (Eds.: H. Kuzmany, J. Fink, M. Mehring, S. Roth), Amer Inst Physics, Melville, **1998**, p. 363.
[17] a) K. Komatsu, M. Murata, Y. Murata, *Science* **2005**, *307*, 238; b) Y. Murata, M. Murata, K. Komatsu, *J. Am. Chem. Soc.* **2003**, *125*, 7152.
[18] a) S. Iwamatsu, T. Uozaki, K. Kobayashi, S. Y. Re, S. Nagase, S. Murata, *J. Am. Chem. Soc.* **2004**, *126*, 2668; b) K. Kurotobi, Y. Murata, *Science* **2011**, *333*, 613.
[19] a) W. A. de Heer, D. Ugarte, *Chem. Phys. Lett.* **1993**, *207*, 480; b) F. Tian, J. C. An, H. M. Cao, S. Z. Guo, J. Zhao, X. Z. Lu, *J. Nanosci. Nanotechnol.* **2013**, *13*, 4468; c) D. Ugarte, *Nature* **1992**, *359*, 707.
[20] a) W. Li, D. Chen, Z. Li, Y. Shi, Y. Wan, J. Huang, J. Yang, D. Zhao, Z. Jiang, *Electrochem. Commun.* **2007**, *9*, 569; b) W. Li, D. Chen, Z. Li, Y. Shi, Y. Wan, G. Wang, Z. Jiang, D. Zhao, *Carbon* **2007**, *45*, 1757; c) S. B. Yoon, K. Sohn, J. Y. Kim, C. H. Shin, J. S. Yu, T. Hyeon, *Adv. Mater.* **2002**, *14*, 19.
[21] a) M. Li, Q. Wu, M. Wen, J. Shi, *Nanoscale Res. Lett.* **2009**, *4*, 1365; b) K. Tang, L. J. Fu, R. J. White, L. H. Yu, M. M. Titirici, M. Antonietti, J. Maier, *Adv. Energy Mater.* **2012**, *2*, 873; c) R. J. White, K. Tauer, M. Antonietti, M. M. Titirici, *J. Am. Chem. Soc.* **2010**, *132*, 17360; d) H. J. Zhang, X. Li, *J. Colloid Interface Sci.* **2015**, *452*, 141.
[22] a) J.-M. Du, D.-J. Kang, *Mater. Res. Bull.* **2006**, *41*, 1785; b) T. K. Ellis, C. Paras, M. R. Hill, J. A. Stride, *Aust. J. Chem.* **2013**, *66*, 1435; c) S. Y. Sawant, R. S. Somani, B. L. Newalkar, N. V. Choudary, H. C. Bajaj, *Mater. Lett.* **2009**, *63*, 2339.
[23] A. H. Lu, T. Sun, W. C. Li, Q. Sun, F. Han, D. H. Liu, Y. Guo, *Angew. Chem. Int. Ed.* **2011**, *50*, 11765; *Angew. Chem.* **2011**, *123*, 11969.
[24] A. Nieto-Márquez, R. Romero, A. Romero, J. L. Valverde, *J. Mater. Chem.* **2011**, *21*, 1664.
[25] a) E. K. Athanassiou, R. N. Grass, W. J. Stark, *Nanotechnology* **2006**, *17*, 1668; b) F. M. Koehler, N. A. Luechinger, D. Ziegler, E. K. Athanassiou, R. N. Grass, A. Rossi, C. Hierold, A. Stemmer, W. J. Stark, *Angew. Chem. Int. Ed.* **2009**, *48*, 224; *Angew. Chem.* **2009**, *121*, 230.
[26] R. N. Grass, E. K. Athanassiou, W. J. Stark, *Angew. Chem. Int. Ed.* **2007**, *46*, 4909; *Angew. Chem.* **2007**, *119*, 4996.
[27] C. J. Hofer, V. Zlateski, P. R. Stoessel, D. Paunescu, E. M. Schneider, R. N. Grass, M. Zeltner, W. J. Stark, *Chem. Commun.* **2015**, *51*, 1826.
[28] F. M. Koehler, W. J. Stark, *Acc. Chem. Res.* **2013**, *46*, 2297.
[29] C. M. Schumacher, R. N. Grass, M. Rossier, E. K. Athanassiou, W. J. Stark, *Langmuir* **2012**, *28*, 4565.
[30] a) D. Avnir, D. Levy, R. Reisfeld, *J. Phys. Chem.* **1984**, *88*, 5956; b) K. Kemnitz, N. Tamai, I. Yamazaki, N. Nakashima, K. Yoshihara, *J. Phys. Chem.* **1986**, *90*, 5094.
[31] a) C. Y. Gao, E. Donath, H. Möhwald, J. C. Shen, *Angew. Chem. Int. Ed.* **2002**, *41*, 3789; *Angew. Chem.* **2002**, *114*, 3943; b) X. Y. Liu, C. Y. Gao, J. C. Shen, H. Möhwald, *Macromol. Biosci.* **2005**, *5*, 1209.
[32] J. L. Benoit-Guyod, J. Rochat, J. Alary, C. Andre, G. Taillandier, *Toxicol. Eur. Res.* **1979**, *2*, 241.
[33] K. S. W. Sing, D. H. Everett, R. A. W. Haul, L. Moscou, R. A. Pierotti, J. Rouquerol, T. Siemieniewska, *Pure Appl. Chem.* **1985**, *57*, 603.
[34] a) H. Giesche, *Part. Part. Syst. Charact.* **2006**, *23*, 9; b) R. L. Portsmouth, L. F. Gladden, *Chem. Eng. Sci.* **1991**, *46*, 3023.
[35] a) A. J. Khopade, F. Caruso, *Biomacromolecules* **2002**, *3*, 1154; b) X. Liu, H. Jiang, W. Ge, C. Wu, D. Chen, Q. Li, Y. Chen, X. Wang, *RSC Adv.* **2015**, *5*, 17532; c) J. Zhu, L. Liao, X. J. Bian, J. L. Kong, P. Y. Yang, B. H. Liu, *Small* **2012**, *8*, 2715.

Received: March 18, 2016
Published online: June 13, 2016

